SERBIAN JOURNAL OF ELECTRICAL ENGINEERING
Vol. 15, No. 3, October 2018, 301-317

UDC: 621.391 **DOI: https://doi.org/10.2298/SJEE1803301I**

An Unequal Error Protection Scheme for Non-Binary LDPC using Statistical QAM and Prioritized Mapping

Madhavsingh Indoonundon[1], Tulsi Pawan Fowdur[2]

Abstract: Low Density Parity Check (LDPC) codes are among the most popular channel codes used nowadays because of their ability to achieve near channel capacity performances. However, with the ever-increasing demand for reliable transmission of data at higher data rates, there is a need to narrow down the gap between the performance of LDPC codes and the channel capacity. LDPC codes and Quadrature Amplitude Modulation (QAM) have been widely deployed in wireless communication standards such as the IEEE 802.11n and Digital Video Broadcasting-Second Generation Terrestrial (DVB-T2). Recently, several Unequal Error Protection (UEP) schemes have been used to enhance the performance of LDPC codes. In this paper an UEP scheme is proposed for Non-Binary LDPC codes with QAM. The scheme uses the statistical distribution of the source symbols to obtain a more efficient statistical QAM constellation. Additionally, it uses the degree distribution of the nodes of the LDPC codeword to achieve prioritized QAM mapping. Simulations revealed that the proposed scheme can provide E_b/N_0 gains of up to 0.78 dB and 1.24 dB with 16-QAM and 64-QAM respectively in the range BER$\leq 10^{-2}$.

Keywords: Unequal Error Protection, Non-Binary, Low Density Parity Check, IEEE 802.11n, Quadrature Amplitude Modulation.

1 Introduction

LDPC codes are Forward Error Correction codes which were invented by Gallagher in 1962 [1]. However, they were ignored due to their computational complexity but were then re-introduced in 1996 by Mackay and Neal [2]. In 1998 Mackay and Neal also came up with Non-Binary LDPC (NB-LDPC) codes which could provide a better performance than LDPC codes [3]. Since they can achieve near Shannon limit performances, LDPC codes are considered to be among the most powerful error correcting codes developed to date [4]. LDPC codes are used in several communications standards such as WiMax [5],

[1]Department of Electrical and Electronic Engineering, University of Mauritius, Reduit, Mauritius;
E-mail: madhavsingh.indoonundon@umail.uom.ac.mu
[2]Department of Electrical and Electronic Engineering, University of Mauritius, Reduit, Mauritius;
E-mail: p.fowdur@uom.ac.mu

DVB-T2 [6] and IEEE 802.11n [7]. The IEEE 802.11n standard consists of QAM combined with LDPC codes and uses code lengths ranging from 648 to 1944 bits, and code rates ranging from 5/6 to 1/2 [7, 8]. Various recent papers have shown that the use of UEP can provide significant performance gains with LDPC codes. An overview of UEP schemes developed for LDPC codes as well as schemes which make use of NB-LDPC codes to enhance the performance of systems is given next.

UEP can be performed on QAM constellations by the bit-reordering scheme proposed in [9]. The authors [9] combined LTE Turbo codes with QAM and then UEP was used to protect the systematic bits more than the parity bits. This provided significant performance gains [9]. In [10], the authors extended the work of [9] with joint source channel decoding for LTE Turbo codes. The same UEP principle was applied to IEEE 802.11n LDPC codes along with a modified hybrid ARQ scheme in [11]. In [12], UEP was used with schemes such as Optimized Scaling Factor (OSF) and Failed Check Nodes (FCN) to enhance the overall error performance. In [13], a scheme was introduced whereby UEP was performed by mapping the more important bits of an image to the variable nodes with higher degrees in irregular LDPC codes. After performing LDPC encoding, the parity check bits were mapped onto a spectrally efficient 16-QAM constellation and systematic bits were mapped onto a power efficient QAM constellation. The scheme provided significant performance gains [13]. Additionally, in a NB-LDPC coded modulation system, the authors of [14] employed an UEP scheme based on the principle of bit reliability. At a BER of 10^{-5}, the scheme achieved a gain between 0.1 to 0.5 dB [14]. In [15], the complexity of the Belief-Propagation algorithm for NB-LDPC decoding was reduced by incorporating FFT at the horizontal step. A hybrid of the Belief-Propagation algorithm and the Most Reliable Basis algorithm for NB-LDPC decoding was proposed in [16] for improving error performance but at the cost of a slight increase in complexity. NB-LDPC codes were concatenated with Reed-Solomon (RS) codes in [17] to lower the error floor of the iterative double-reliability-based majority-logic decoding (IDRB-MLGD) algorithm. First, the IDRB-MLGD algorithm was used to decode the NB-LDPC codeword and then remaining errors were set into RS code blocks which were decoded using a low-complexity RS decoder to further reduce the amount of errors. In [18], a statistical QAM based modulation scheme for low complexity video transmission was proposed. The rationale behind the scheme was to map the most frequent pixel values onto the QAM constellation points with the lowest energy. Consequently, the average energy needed for image transmission was much smaller and allowed for increasing the spacing between QAM constellation points for the same average energy thus improving the BER [18]. Finally, in [19], a novel hybrid UEP scheme was proposed for LDPC codes with QAM. The scheme used the statistical distribution of the source symbols to map

the systematic bits of the LDPC encoded symbols on the QAM constellation. Essentially, systematic symbols having highest probabilities of occurrence are mapped onto the low power region of the QAM constellation and those with low probability of occurrence are mapped onto the high power region. The decrease in overall transmission power allows for an increased spacing between the QAM constellation points. Additionally, the scheme used the distribution of the bit nodes' degree of the LDPC codeword to map the parity bits having the highest degree onto prioritized QAM constellation points.

In this paper, the hybrid UEP scheme of [19] is extended to NB-LDPC codes. In general the hybrid UEP scheme combines the concepts of statistical QAM, prioritized constellation mapping and uneven degree distribution of variable nodes with LDPC codes. To employ the scheme with NB-LDPC, the UEP reordering process was modified so that it can be used with Galois-field symbols instead of bits. Simulations are performed with the IEEE 802.11n LDPC codes parity check matrices. Results showed that the proposed hybrid scheme can provide gains ranging from 0.58 dB to 1.24 dB in E_b/N_0 for code rates of 1/2, 2/3 and 3/4 as compared with other UEP schemes for a range of Bit Error Rate (BER) values. Compared with LDPC codes of [19], when the proposed UEP scheme is applied to NB-LDPC codes, additional gains of up to 0.17 dB and 0.22 dB are obtained when using 16-QAM and 64-QAM respectively.

This paper is structured as follows. Section 2 gives the transmitter and receiver system models with the hybrid UEP scheme. Section 3 presents the simulation results and analysis. Section 4 concludes the paper.

2 Transmitter and Receiver Systems for UEP with Non-Binary LDPC codes

2.1 Transmitter

The block diagram of the transmitter is shown in Fig. 1. It is based on the transmitter proposed in [19] with the exception that NB-LDPC has been used in this case. Only one of the two optional multiplexing modes labelled as "Mode 1" and "Mode 2" is used at a time, depending on which mode is selected.

A random alphabet source inputs data not having an equiprobable probability distribution. Table 1 gives the probabilities of the alphabet present in the alphabet source. Variable length coding (VLC), such as Huffman coding, is then performed on the generated alphabet to assign codewords to them. Table 1 gives an example of Huffman codes assigned to a list of alphabet with respect to their probabilities [20].

The alphabet in the stream are fitted into packets such that the number of bits obtained after performing VLC on the alphabet in each packet is equal to the number of systematic bits required for NB-LDPC encoding [19].

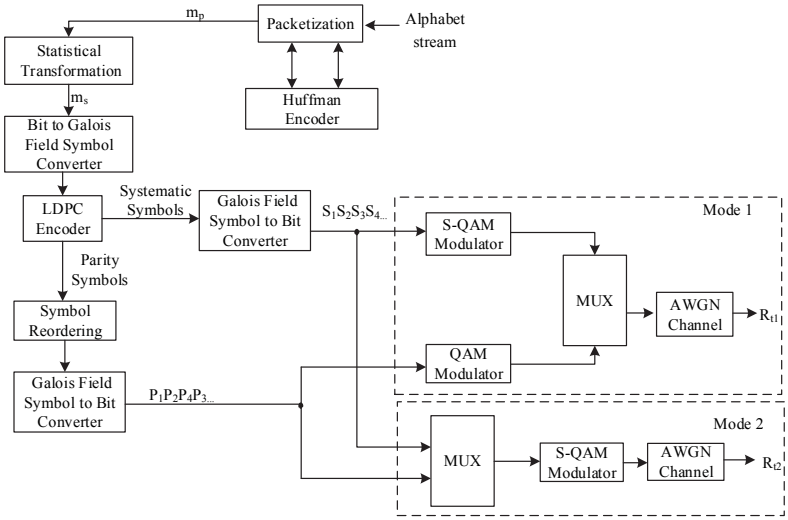

Fig. 1 – *Transmitter with statistical QAM transformation and bit reordering [19].*

Table 1
The alphabet source and their VLC codewords.

Alphabet	Probability	Codeword
a	0.4	00
b	0.25	10
c	0.2	11
d	0.1	011
e	0.05	010

S-QAM (Statistical QAM) mapping is then performed on the message bit-stream using the same method as in [19]. The block of message bits in each packet is labelled as m_p. With S-QAM, the a-priori probabilities of the QAM symbols are derived by first obtaining the a-priori probabilities of systematic bit 1 and 0 from Table 1. The statistically transformed block of bits is labelled as m_s.

Table 2 gives the probabilities of the whole set of QAM symbols when 16-QAM is used [19].

The probabilities of the message symbols are then used to generate the S-QAM transformation lookup table in the statistical transformation block [19]. This block transforms the most probable symbols obtained from m_p to the lowest power symbols and the least probable ones into the highest power symbols, hence reducing the overall transmission power [19]. The S-QAM transformation table for the considered case is the same as in [19] and is given in Table 2.

Table 2
S-QAM transformation lookup table [19].

Initial Symbol	Probability	Transformed Symbol
0000	0.1226	1111
0001	0.0846	0001
0010	0.0846	0101
0011	0.0584	0011
0100	0.0846	1101
0101	0.0584	0100
0110	0.0584	0110
0111	0.0403	1110
1000	0.0846	0111
1001	0.0584	1001
1010	0.0584	1011
1011	0.0403	0000
1100	0.0584	1100
1101	0.0403	0010
1110	0.0403	1000
1111	0.0278	1010

The proposed system leads to an increase in complexity as it requires a statistical QAM transformation at the transmitter side. The look-up table for the S-QAM transformation can in fact be pre-computed before data transmission to minimize the transmission delay. A slight increase in complexity is also brought about by the symbol re-ordering and multiplexing blocks. However, the overall increase in computational complexity is acceptable as it does not lead to significant transmission delays.

Then, for GF(2^k) NB-LDPC code encoding of m_s, each set of k bits in m_s must first be converted to GF(2^k) elements and then encoded using (1) with GF(2^k) arithmetic.

$$\boldsymbol{c} = \boldsymbol{u}\boldsymbol{G}\,, \tag{1}$$

where,

$\boldsymbol{c}$ is the NB-LDPC codeword;

$\boldsymbol{u}$ is the message row vector and

$\boldsymbol{G}$ is the NB-LDPC generator matrix.

In this work, the generator matrix used is as per the IEEE 802.11n LDPC codes [8].

Note that a NB-LDPC matrix over GF(q) may be constructed from the IEEE 802.11n LDPC matrix by simply replacing every non-zero elements in the LDPC matrix with randomly selected elements of the GF(q) [21]. A section of the IEEE 802.11n LDPC matrix converted to a GF(16) NB-LDPC matrix is shown next:

LDPC matrix → NB-LDPC matrix

$$\begin{pmatrix} \cdots & 1 & 0 & 0 & 0 & \cdots \\ \cdots & 0 & 1 & 0 & 0 & \cdots \\ \cdots & 0 & 0 & 1 & 0 & \cdots \\ \cdots & 0 & 0 & 0 & 1 & \cdots \\ \cdots & \vdots & \vdots & \vdots & \vdots & \ddots \end{pmatrix} \rightarrow \begin{pmatrix} \cdots & 4 & 0 & 0 & 0 & \cdots \\ \cdots & 0 & 10 & 0 & 0 & \cdots \\ \cdots & 0 & 0 & 1 & 0 & \cdots \\ \cdots & 0 & 0 & 0 & 7 & \cdots \\ \cdots & \vdots & \vdots & \vdots & \vdots & \ddots \end{pmatrix}$$

After the NB-LDPC encoding process, the NB-LDPC codeword is converted back to the binary form for modulation and transmission

The parity symbols of NB-LDPC codeword are reordered so that they can benefit from UEP due to a prioritized mapping in the QAM constellation. The reordering is performed based on the degree distribution of the parity variable nodes [14]. Basically, variable nodes which have higher degrees are given more protection than those with lower degrees by placing them onto prioritized constellation points [19]. For NB-LDPC, the bit reordering process from [19] is modified to perform the reordering of GF symbols instead of bits. In the modified process matrix $\boldsymbol{A}_2$ and $\boldsymbol{A}_3$ have GF symbols in the last row as shown below:

$$A_2 = \begin{bmatrix} \cdots & 347 & 348 & 349 & 350 & 351 & 352 & 353 & 354 & 355 & 356 & 357 & 358 & \cdots \\ \cdots & 3 & 3 & 3 & 3 & 3 & 2 & 2 & 2 & 2 & 2 & 2 & 2 & \cdots \\ \cdots & 1 & 4 & 0 & 10 & 6 & 0 & 0 & 15 & 0 & 0 & 2 & 11 & \cdots \end{bmatrix} \leftarrow \text{GF Symbols}$$

$$A_3 = \begin{bmatrix} \cdots & 352 & 353 & 354 & 355 & 356 & 357 & 358 & 347 & 348 & 349 & 350 & 351 & \cdots \\ \cdots & 2 & 2 & 2 & 2 & 2 & 2 & 2 & 3 & 3 & 3 & 3 & 3 & \cdots \\ \cdots & 0 & 0 & 15 & 0 & 0 & 2 & 11 & 1 & 4 & 0 & 10 & 6 & \cdots \end{bmatrix} \leftarrow \text{GF Symbols}$$

LP HP

Reordering of the symbols is performed such that the highest priority symbols are given maximum protection by placing them on prioritized constellation points as explained next [10]. The symbols are first converted to bits prior to performing the following reordering process.

2.1.1 Mode 1 Multiplexing

After the reordering process, when using Mode 1, the bits corresponding to systematic symbols are modulated using S-QAM and those corresponding to parity symbols are modulated using the conventional Gray-coded QAM. For S-QAM, the separation distance between the constellation points, d_s for the S-

QAM constellation is the same as that in [19] and is given in Table 3 for both 16 and 64 QAM for the Mode 1.

Table 3

Calculated values of d_s for different cases using Mode 1 [19].

QAM Order (*M*)	d_s
16	2.37
64	2.59

Fig. 2 shows the difference between a conventional QAM constellation ($d_s = 2$) and the S-QAM constellation obtained for 16-QAM.

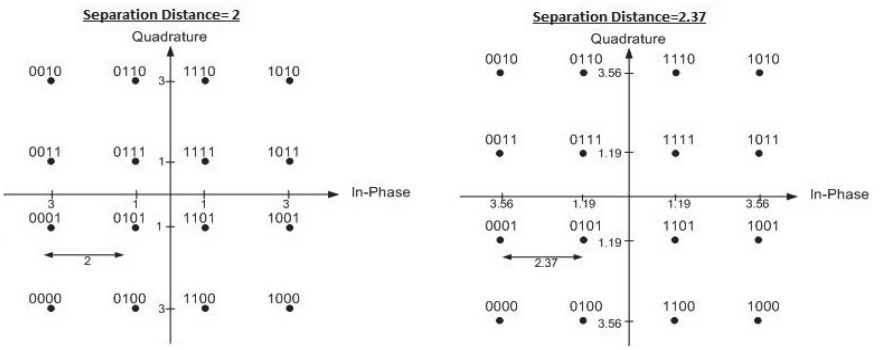

Fig. 2 – *Comparison of constellations of different values of d_s.*

2.1.2 Mode 2 Multiplexing

Table 4

Calculated values of ds for different cases using Mode 2 [19].

QAM Order	Code-Rate (*R*)	d_s
16	1/2	2.17
16	2/3	2.23
16	3/4	2.26
64	1/2	2.31
64	2/3	2.40
64	3/4	2.44

For Mode 2, the values of d_s for the different LDPC code-rates and QAM modulation orders are calculated using the same method as for Mode 1 but with the probabilities of the QAM symbols obtained from the whole codeword [19]. Table 4 contains the values of d_s obtained for 16 and 64 QAM with different code-rates for Mode 2 as calculated in [19].

2.1.3 Separation distance with Mode 1 and Mode 2 Multiplexing

It is observed from **Tables 3** and **4** that in Mode 1, the values of d_s are obtained larger than in Mode 2 due to the exclusion of parity bits in S-QAM, hence leading into an improved protection of the systematic bits. On the other hand, in Mode 2, where the values of d_s are lower than in Mode 1 but which are still higher than in conventional Grey Coded QAM, provides the S-QAM protection to both parity and systematic bits.

The modulated signal is then transmitted over the AWGN channel to the receiver.

2.2 Receiver

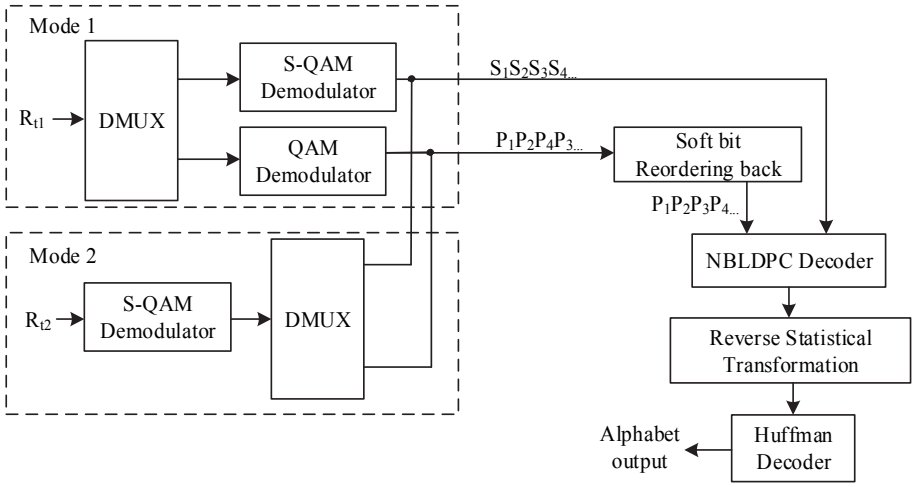

Fig. 3 – *Block diagram of receiver system [19].*

2.2.1 Mode 1 De-multiplexing

When operating in Mode 1, the received QAM symbols, R_t, are first de-multiplexed into the systematic and parity symbols. The S-QAM demodulator is then used to demodulate the systematic symbols and the conventional QAM demodulator is used to demodulate the parity symbols, as shown in Fig. 3.

2.1.3 Mode 2 De-multiplexing

In Mode 2, the S-QAM demodulator is first used to demodulate R_t which is then de-multiplexed into the systematic and parity parts.

2.2.3 Bit-reordering process

Soft bit reordering is performed to reorder back the parity soft bits into their original positions prior to sending them to the NB-LDPC decoder with the systematic soft bits.

2.2.4 NB-LDPC decoding process

NB-LDPC decoding is then performed using the Fast-Fourier-Transform based Sum-Product Algorithm (FFT-SPA) which can be summarized as follows [22]:

Step 1: Initialization Step

The probabilities that the n-th received bit in a codeword is binary 0 or 1 are obtained by using (2) and (3) respectively.

$$g_n^{(0)} = \frac{1}{1 + e^{\left(\frac{-2r_n}{\sigma^2}\right)}}, \tag{2}$$

$$g_n^{(1)} = \frac{1}{1 + e^{\left(\frac{2r_n}{\sigma^2}\right)}}, \tag{3}$$

where,

r_n is the n^{th} demodulated bit and

σ is the noise distribution's standard deviation.

For GF(q), the probability of each q symbols is the product of each demodulated bits which constitute the symbol [22]. For example, when GF(2^4) is used, every consecutive 4 bits make up one Galois field element. The probability that the first 4 bits in the codeword make up the GF(2^4) symbol '5' (0101 in binary) is computed as follows:

$$f_1^{(0101)} = g_1^{(0)} \times g_2^{(1)} \times g_3^{(0)} \times g_4^{(1)}. \tag{4}$$

A matrix Q, containing values for probabilities $q_{mn}(x)$ is initialized. $q_{mn}(x)$ is the probability of the n-th Galois field symbol is x given that the parity checks linked to it excluding the m-th parity check are satisfied [22]. For all non-zero positions (m, n) in H:

$$q_{mn}(x) = f_n^{(x)}. \tag{5}$$

Otherwise, at zero positions (m, n) in H, $q_{mn}(x) = 0$.

Step 2: Permutation Step

Each element in each column vector of likelihood in matrix Q are cyclically shifted downwards except the elements corresponding to the probabilities of the coded symbol being zero. The number of cyclic shifts is equal to the power of

the primitive element in the parity check matrix that is multiplied with the coded symbol [23].

Step 3: Horizontal Step

In this step, each check node *m* is updated using the channel reliability message from adjacent variable nodes except this check node m [23] as follows:

$$r_{mn}(x) = F^{-1}\left(\prod_{n\in\frac{Nm}{n}}\left(F\left(q_{mn'}(x)\right)\right)\right), \tag{6}$$

where,

F is the Fourier transform and

F^{-1} is the inverse Fourier transform.

Step 4: Depermutation Step

The inverse of Step 2 is performed by cyclically shifting downwards each element in each column vector of likelihood. The elements corresponding to the probabilities of the coded symbol being zero are not involved in the process.

Step 5: Vertical Step

In this step, variable node *n* is updated adjacent check node's message. The message transfer from the check node to the variable node is found as follows [23]:

$$q_{mn}(x) = \beta_{mn} f_n^x \prod_{m'\in\frac{M_n}{m}} r_{m'n}(x), \tag{7}$$

where,

$$\beta_{mn} = \frac{1}{\sum_x f_n^x \prod_{m'\in\frac{M_n}{m}} r_{m'n}(x)}. \tag{8}$$

Then the pseudo posterior probabilities $q_n(x)$ are calculated as follows [23]:

$$q_n(x) = \beta_n f_n^x \prod_{m'\in M_n} r_{mn}(x), \tag{9}$$

where,

$$\beta_n = \frac{1}{\sum_x f_n^x \prod_{m'\in M_n} r_{mn}(x)}. \tag{10}$$

Using $q_n(x)$, the transmitted codeword can be estimated as [23]:

$$\hat{c}_n = \arg\max_x q_n(x). \tag{11}$$

If the syndrome calculated using $\hat{c}_n$ and H is not 0, the next iteration which begins with the horizontal step using the updated Q matrix is performed until either the maximum iteration is reach or until the syndrome becomes 0 [23].

The decoded systematic bits is sent to the Statistical De-mapping block whereby they are grouped into blocks of $\log_2(M)$ consecutive bits. The inverse S-QAM transformation is then performed as per the statistical transformation, lookup Table 2**,** so that the message bit-stream is recovered.

Finally, the message bit-stream is decoded using a VLC decoder to recover the alphabet stream.

3 Results and Discussion

In order to observe the extent by which the proposed hybrid scheme is able to enhance the performance of the IEEE 802.11n LDPC codes, the scheme was implemented on MATLAB® R2013a to assess its performance through simulations. The MATLAB model used is based on Monte Carlo Simulations. It consists of a series of m-files and functions for simulating the different blocks of the transmitter and receiver systems given in Figs. 1 and 3. The alphabet were generated randomly and the average BERs obtained from several simulations at each E_b/N_0 were used the plot all graphs. The simulations have been performed mainly to observe performance in the waterfall region as in [19].

The schemes tested are similar to those in [19] but with NB-LDPC and different multiplexing methods. These are given in **Table 5**:

Table 5

Simulated schemes.

Scheme	Description
1	NB-LDPC codes with S-QAM and UEP using Mode 1 multiplexing.
2	NB-LDPC codes with S-QAM and UEP using Mode 2 multiplexing.
3	NB-LDPC codes with S-QAM using Mode 1 multiplexing.
4	NB-LDPC codes with S-QAM using Mode 2 multiplexing.
5	Conventional QAM with UEP involving bit reordering of both systematic and parity symbols.
6	Conventional NB-LDPC encoding and decoding with conventional QAM and without UEP.

In all of these schemes, a total of 476191 alphabet were packetised and transmitted. The code-length used for all the schemes is 648 GF symbols.

3.1 Simulation Results using NB-LDPC codes with 16-QAM

The graphs of BER against E_b/N_0 for the six schemes using NB-LDPC codes of different code-rates with 16-QAM are shown in Fig. 4 – 6.

It is observed from the graphs in Fig. 4 – 6 that scheme 2 slightly outperforms scheme 1 by 0.1 dB with code-rates 1/2 and 2/3 in the range $10^{-3} \leq \text{BER} \leq 10^{-4}$ and when R=3/4, scheme 2 is found to converge with scheme 1.

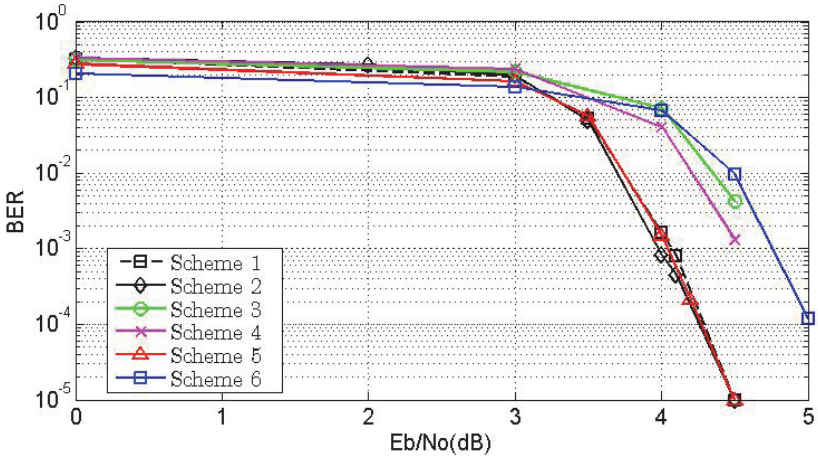

Fig. 4 – *BER performance of schemes using 16-QAM with NB-LDPC codes and R=1/2.*

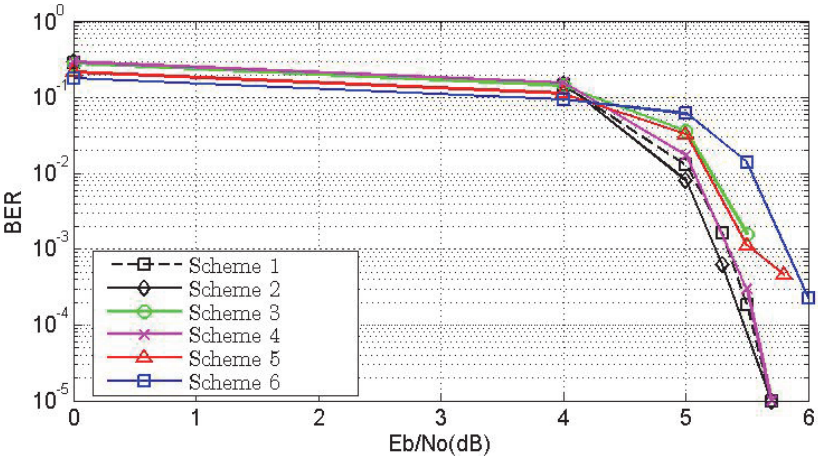

Fig. 5 – *BER performance of schemes using 16-QAM with NB-LDPC codes and R=2/3.*

Scheme 2 provides significant gains of 0.78 dB, 0.58 dB and 0.6 dB over scheme 6 with code-rates 1/2, 2/3 and 3/4 respectively in the range $10^{-2} \leq \text{BER} \leq 10^{-4}$. However, the hybrid scheme with both modes does not provide gains with BER values greater than 10^{-2}. This is because with statistical transformation, if one bit is in error, the whole transformed symbol of 4 bits is

transformed to a wrong initial symbol during the inverse S-QAM transformation process.

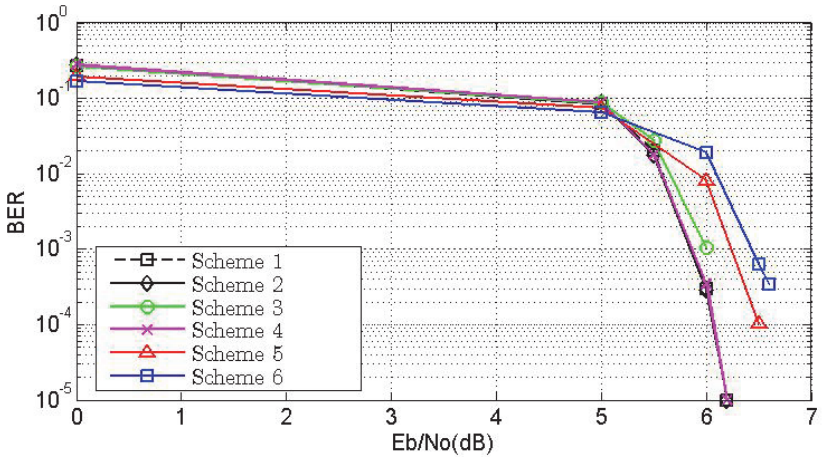

Fig. 6 – *BER performance of schemes using 16-QAM with NB-LDPC codes and R=3/4.*

3.2 Simulation Results using NB-LDPC codes with 64-QAM

The graphs of BER against E_b/N_0 for the six schemes using NB-LDPC codes of different code-rates with 64-QAM are shown in Fig. 7 – 9.

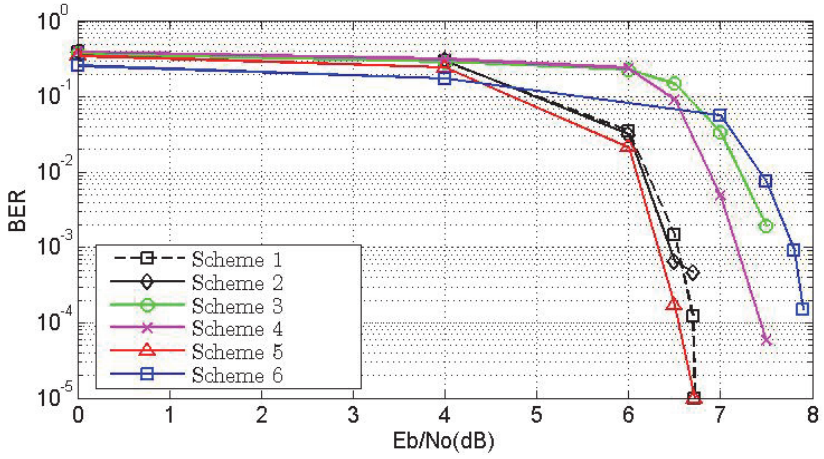

Fig. 7 – *BER performance of schemes using 64-QAM with NB-LDPC codes and R=1/2.*

From the results obtained in Fig. 7 – 9, it is found that scheme 5 gives larger gains over scheme 6 compared to when LDPC is used, as observed in [19]. This may be because with NB-LDPC, as the codeword contains more bits

and that each variable node degrees may be considered to be shared with every 4 bits constituting the node, more variation in degree is obtained and this makes the UEP scheme perform better. Scheme 5 is also found to outperform the proposed hybrid scheme in both modes by approximately 0.2 dB when code-rate 1/2 is used. The two modes of the hybrid scheme provide almost similar performances over the whole E_b/N_0 range. They provide significant gains of 1.24 dB, 1.05 dB and 1 dB over scheme 6 in the range $10^{-2} \leq \text{BER} \leq 10^{-4}$ with code-rates 1/2, 2/3 and 3/4 respectively.

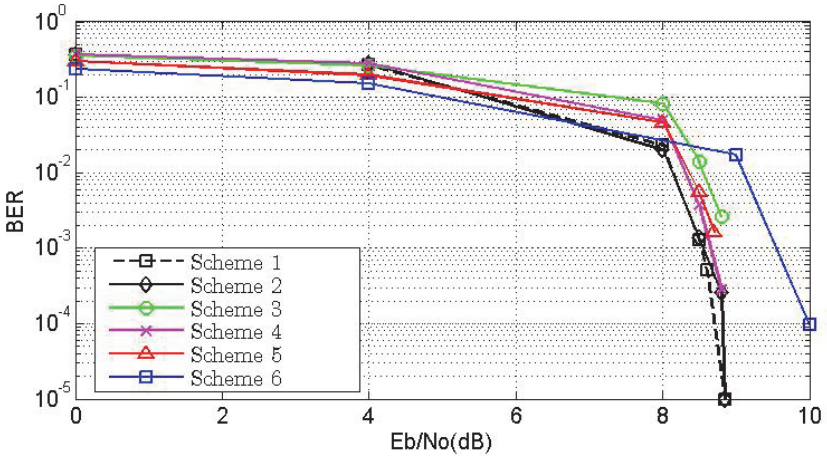

Fig. 8 – *BER performance of schemes using 64-QAM with NB-LDPC codes and R=2/3.*

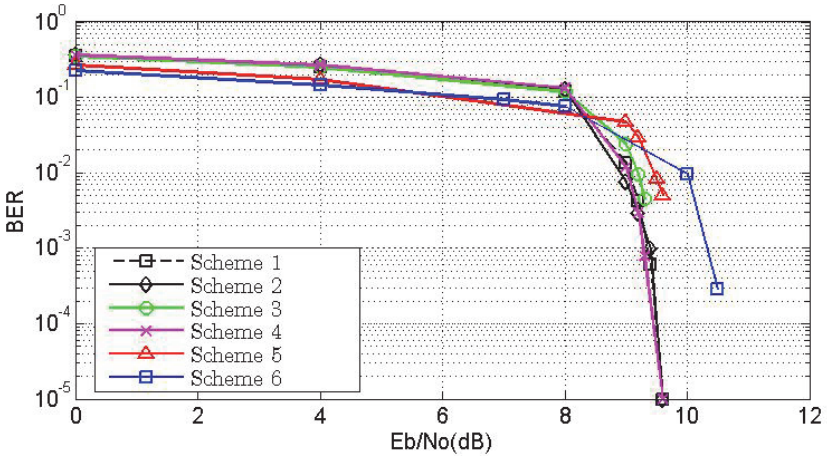

Fig. 9 – *BER performance of schemes using 64-QAM with NB-LDPC codes and R=3/4.*

3.3 Performance Comparison of UEP schemes with NB-LDPC and LDPC codes

Fig. 10 shows the performances of schemes 1 and 2 with NB-LDPC and LDPC from [19] when using 16-QAM and 64-QAM with LDPC code-rate 3/4. The code-lengths used for LDPC and NB-LDPC are 648 bits and 648 GF symbols respectively.

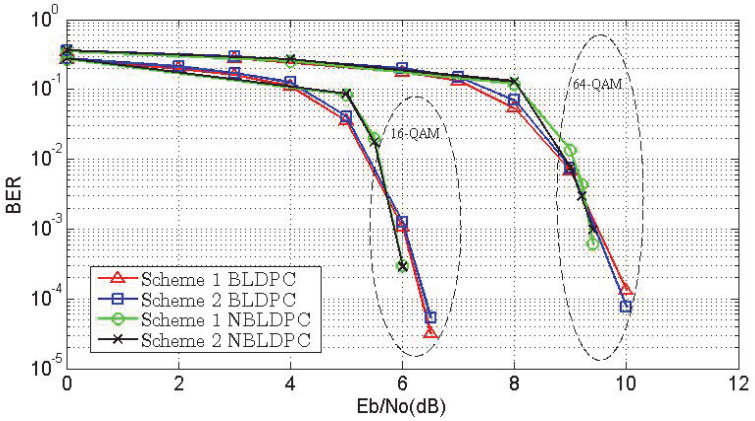

Fig. 10 – *Comparison between LDPC and NB-LDPC codes results with R=3/4.*

It is observed from Fig. 10 that both schemes 1 and 2 with NB-LDPC codes outperform those with LDPC codes with gains which increases with decreasing BER. This may be due to the enhanced performance that NB-LDPC inherently provides over LDPC [3]. A gain of up to 0.17 dB is observed in the region BER$\leq 10^{-3}$ with 16-QAM. With 64-QAM, a similar trend is observed. The schemes with NB-LDPC codes outperform their LDPC codes counterparts with gains which increase with decreasing BER as seen in Fig. 10. In the region BER$\leq 10^{-3}$, scheme 1 with NB-LDPC codes provides a maximum gain of 0.22 dB over scheme 1 with NB-LPDC codes over scheme 1 with LDPC codes and scheme 2 with NB-LDPC codes provides a maximum gain of 0.05 dB over scheme 2 with LDPC codes.

4 Conclusion

This paper proposed an enhanced UEP scheme for IEEE 802.11n with NB-LDPC codes by extending the work of [18]. The proposed scheme with NB-LDPC codes was devised by modifying the binary parity check matrix of the IEEE 802.11n LDPC code. Also, the re-ordering process was modified so that Galois-field symbols could be considered instead of bits. Simulations were performed with NB-LDPC with 16 and 64 QAM. With NB-LDPC codes modulated using 16-QAM, the UEP scheme provided a maximum gain of

0.78dB in E_b/N_0 in the range $10^{-2} \leq BER \leq 10^{-4}$ and when modulated using 64-QAM, a maximum gain of 1.24 dB in E_b/N_0 was obtained in the same BER region. Simulations results also showed that the UEP scheme works better with NB-LDPC codes than with LDPC codes in the region $BER \leq 10^{-3}$, providing gains of up to 0.17 dB with 16-QAM and 0.22 dB with 64-QAM over the LDPC codes counterpart. An interesting future work would be to extend the performance analysis with other modulation schemes and LDPC decoding algorithms.

5 References

[1] R. G. Gallager: Low-Density Parity-Check Codes, IRE Transactions on Information Theory, Vol. 8, No. 1, 1962, pp. 21 – 28.

[2] D. J. C. MacKay, R. M. Neal: Near Shannon Limit Performance of Low Density Parity Check Codes, Electronics Letters, Vol. 32, No. 18, 1996, pp. 1645.

[3] M. C. Davey, D. J. C. MacKay: Low Density Parity Check Codes over GF(q), Proceedings of the 1998 IEEE Information Theory Workshop, Killarney, Ireland, June 1998, pp. 70 – 71.

[4] S.- Y. Chung, G. D. Forney, T. J. Richardson, R. Urbanke: On the Design of Low-Density Parity-Check Codes within 0.0045 dB of the Shannon Limit, IEEE Communications Letters, Vol. 5, No. 2, February 2001, pp. 58 – 60.

[5] IEEE 802.16e Task Group (Mobile WirelessMAN),

Available at: http://www.ieee802.org/16/tge/

[6] Digital Video Broadcasting (DVB); Implementation Guidelines for a Second Generation Digital Terrestrial Television Broadcasting System (DVB – T2), ETSI TS 102 831 V1.2.1 (2012-08), Available at:

http://www.etsi.org/deliver/etsi_ts/102800_102899/102831/01.02.01_60/ts_102831v010201p.pdf

[7] IEEE 802.11n-2009 Standard,

Available at: https://standards.ieee.org/

[8] IEEE 802.11n. Wireless LAN Medium Access Control and Physical Layer specifications: Enhancements for Higher Throughput, IEEE P802.16n/D1.0, March 2006.

[9] H. Lüders, A. Minwegen, P. Vary: Improving UMTS LTE Performance by UEP in High Order Modulation, Proceedings of the 7th International Workshop on Multi-Carrier Systems & Solutions (MC-SS 2009), Herrsching, Germany, May 2009, pp. 185 – 194.

[10] T. P. Fowdur, Y. Beeharry, K. M. S. Soyjaudah: Performance of LTE Turbo Codes with Joint Source Channel Decoding, Adaptive Scaling and Prioritised QAM Constellation Mapping, International Journal on Advances in Telecommunications, Vol. 6, No. 3 & 4, July 2013, pp. 143 – 152.

[11] T. P. Fowdur, B. N. Furzun: Performance of IEEE 802.11n LDPC Codes with Modified Reliability Based Hybrid ARQ and Unequal Error Protection, Proceedings of the IEEE EUROCON 2015 – International Conference on Computer as a Tool, Salamanca, Spain, September 2015, pp. 1 – 6.

[12] M. Indoonundon, T. P. Fowdur: Combined Unequal Error Protection and Optimized Scaling for IEEE 802.11n Low Density Parity Check Codes, Journal of Electrical Engineering, Electronics, Control and Computer Science, Vol. 3, No. 7, 2017, pp. 13 – 20.

[13] Y. Zhang, X. Li, H. Yang: Unequal Error Protection in Image Transmission Based on LDPC Codes, International Journal of Signal Processing, Image Processing and Pattern Recognition, Vol. 9, No. 3, March 2016, pp. 1 – 10.

[14] L. Chen, L. Keke, F. Zesong, K. Jinming: A Novel Mapping Scheme in Non-Binary LDPC Coded Modulation System, 2008 11th IEEE International Conference on Communication Technology, Hangzhou, China, November 2008, pp. 225 – 228.

[15] L. Barnault, D. Declercq: Fast Decoding Algorithms for LDPC Codes Over GF(2/sup q/), Proceedings of the 2003 IEEE Information Theory Workshop, Paris, France, March 2003, pp. 70 – 73.

[16] M. Baldi, F. Chiaraluce, N. Maturo, G. Liva, E. Paolini: A Hybrid Decoding Scheme for Short Non-Binary LDPC Codes, IEEE Communications Letters, Vol. 18, No. 12, December 2014, pp. 2093 – 2096.

[17] X. Xin, L. Yichao, G. Satoshi: A Low-Complexity Coding Scheme for Non-Binary LDPC Code Based on IDRB-MLGD Algorithm, 2013 9th International Conference on Information, Communications & Signal Processing, Tainan, Taiwan, December 2013, pp. 1 – 5.

[18] A. Sergeev, A. Turlikov, A. Veselov: Statistical Modulation for Low Complexity Video Transmission, Proceedings of the 11th International Symposium on Wireless Personal Multimedia Communications (WPMC), Lapland, Finland, January 2008.

[19] T. P. Fowdur, M. Indoonundon: A Hybrid Statistical and Prioritised Unequal Error Protection Scheme for IEEE 802.11n LDPC Codes, International Journal of Electrical and Computer Engineering Systems, Vol. 8, No. 1, July 2017, pp. 1 – 9.

[20] Y. Takishima, M. Wada, H. Murakami: Reversible Variable Length Codes, IEEE Transactions on Communications, Vol. 43, No. 2/3/4, Feb/Mar/Apr 1995, pp. 158–162.

[21] X.- Y. Hu, E. Eleftheriou, D. M. Arnold: Regular and Irregular Progressive Edge-Growth Tanner Graphs, IEEE Transactions on Information Theory, Vol. 51, No. 1, 2005, pp. 386 – 398.

[22] R. A. Carrasco, M. Johnston: Non-Binary Error Control Coding for Wireless Communication and Data Storage, John Wiley&Sons, Chichester, UK, 2008, 208 – 212.

[23] J. Patel, N. Chapatwala, M. Patel: FFT Based Sum Product Decoding Algorithm of LDPC Coder for GF(q), 2014 2nd International Conference on Emerging Technology Trends in Electronics, Communication and Networking, Surat, India, December 2014, pp. 1 – 4.